Delft University of Technology

Investigation of buckling response of cylindrical shells using 3D-printing technology

Bisagni, Chiara; Labans, Edgars

Publication date
2022

Document Version
Final published version

Published in
33rd Congress of the International Council of the Aeronautical Sciences, ICAS 2022

Citation (APA)
Bisagni, C., & Labans, E. (2022). Investigation of buckling response of cylindrical shells using 3D-printing technology. In *33rd Congress of the International Council of the Aeronautical Sciences, ICAS 2022* (pp. 3691-3698). (33rd Congress of the International Council of the Aeronautical Sciences, ICAS 2022; Vol. 5). International Council of the Aeronautical Sciences.

Important note
To cite this publication, please use the final published version (if applicable).
Please check the document version above.

Copyright
Other than for strictly personal use, it is not permitted to download, forward or distribute the text or part of it, without the consent of the author(s) and/or copyright holder(s), unless the work is under an open content license such as Creative Commons.

Takedown policy
Please contact us and provide details if you believe this document breaches copyrights.
We will remove access to the work immediately and investigate your claim.

This work is downloaded from Delft University of Technology.
For technical reasons the number of authors shown on this cover page is limited to a maximum of 10.

33RD CONGRESS
OF THE INTERNATIONAL COUNCIL
OF THE AERONAUTICAL SCIENCES
STOCKHOLM, SWEDEN, 4-9 SEPTEMBER, 2022

INVESTIGATION OF BUCKLING RESPONSE OF CYLINDRICAL SHELLS USING 3D-PRINTING TECHNOLOGY

Chiara Bisagni & Edgars Labans

Delft University of Technology, Faculty of Aerospace Engineering, Delft, 2629HS, Netherlands

Abstract

In the current research the buckling response of cylindrical shells manufactured using 3D-printing technology is studied numerically and experimentally. The 3D-printing technology allows quick prototyping in order to assess the influence of the corrugated surface of the shells on the buckling loads. Finite element analyses are conducted using the commercial finite element code Abaqus, and the structural behavior is analyzed up to the post-buckling field. A few shells are manufactured using additive 3D-printing technology and tested in compression. The shells are then optimized in terms of the amplitude of the corrugation and the number of the sinusoidal waves. The average buckling load of the optimized corrugated shells results 160% higher of the buckling load of the cylindrical shells with circular section, keeping the same stiffness and mass. The introduction of the corrugated surfaces, not only significantly improves the buckling load, but also reduces the sensitivity towards initial geometrical imperfections. The knowledge acquired on these small 3D-printed shells can be useful for the design of new aerospace cylindrical shells.

Keywords: buckling, corrugated surface, 3D-printing technology, finite element model, buckling tests

1. Introduction

Several components of aircraft fuselages and space launch vehicles consist of cylindrical shells. As their thickness can be very thin, when loaded in compression, they can be subjected to buckling. Consequently buckling is one of the main design cases when subjected to compressive loads. Different studies can be found in literature on the buckling of composite cylindrical shells for aeronautical and space applications [1-4].

Only recently, shells with corrugated surfaces started to attract attention. Ning and Pellegrino [5-6] conducted numerical and experimental work on waved composite cylindrical shells to design shells insensitive towards geometrical imperfections. Sowiński [7] studied the influence of the shape on barrelled, pseudo-barrelled and cylindrical shells, demonstrating that surface corrugation can increase the load capacity of the shells, and in some cases reduce the sensitivity to the initial imperfections. Other studies can be found in literature that investigated how to reduce the imperfection sensitivity of the shells integrating vertical or horizontal stiffeners [8] or applying variable angle-tow composites [9-10].

Even if large scale 3D-printed shells are not yet feasible mainly because of the manufacturing limitations, some studies on shells made by additive manufacturing can be found in literature as the bio-mimicking of natural structures [11] or folded origami parts with shape memory [12]. Besides, 3-D printed shells have been used recently in laboratory demonstrations for courses teaching stability of structures [13].

Different ways to modify the cylindrical shell geometry can be reached by applying 3D-printing manufacturing technology, which would allow for broader geometrical variations and the local change of the shell thickness [14].

The current study consists of an investigation of the buckling response of 3D-printed cylindrical shells with corrugated surface. Numerical analyses and tests are conducted to study if optimized 3D-printed cylindrical shells with corrugated surface can provide higher buckling loads and can result less sensitivity towards initial geometric imperfections than conventional cylindrical shells.

At first, numerical finite element (FE) analyses are performed using the commercial code Abaqus [15] to analyze and optimize different configurations. Then, a few cylindrical shells are manufactured using 3D-printing technology and are tested in compression. The tests on these small specimens can help to understand the influence of different corrugated shapes before proceeding to investigate larger aerospace structures.

2. Analysis of Conventional Cylindrical Shells and of Corrugated Cylindrical Shells

Conventional cylindrical shells with circular section are initially analyzed. The dimensions of the shells are limited by the available 3D-printing devices, thus the height is assumed equal to 170 mm. Two sets of shell radius are considered, equal to 50 mm and 75 mm. The minimal shell thickness achievable with conventional polymer based 3D-printers is equal to 0.2 mm and the printer nozzle diameter step is 0.1 mm. The shells are made of polylactide (PLA) polymer with modulus of elasticity equal to 2.34 GPa and density equal to 1240 kg/m^3. The plastic yield stress for PLA filament is 46 MPa.

Then, the shell geometry is modified and different shell configurations are manufactured using the 3D-printing technology, as shown in Figure 1. The configuration that is investigated in this study to improve the buckling load, without an increase of the weight respect to the cylindrical shell with circular section, is that one obtained by introducing surface corrugation in the circumferential direction, highlighted in Figure 1, and which top view is shown in Figure 2.

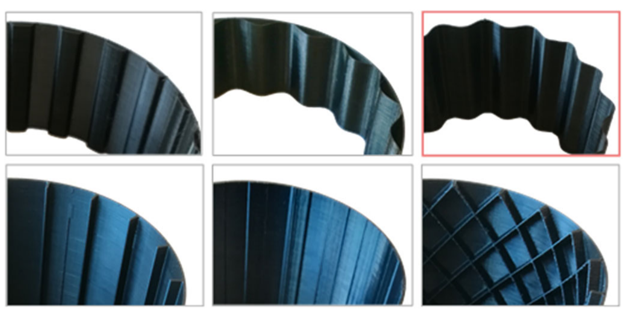

Figure 1 - Different shell configurations manufactured using 3D-printing technology.

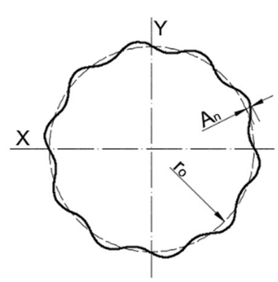

Figure 2 - Top view of corrugated cylindrical shell.

The corrugation is defined by sine wave functions. The amplitude of the corrugation wave along the circumference is indicated with A_n, and the ratio of the amplitude A_n divided by the nominal radius r_0 of the cylindrical shell is indicated with a_n.

Numerical FE analyses are performed using the commercial code Abaqus [14], and the input files for the FE analysis are prepared in MATLAB environment. Conventional S4 shell elements with mesh size of 2 mm are chosen after having conducted a mesh sensitivity study. An example of the FE mesh of a corrugated shell is shown in Figure 3.

The nodes at the bottom-end and at the top-end of the shells are connected with kinematic coupling to two reference nodes. All translations and rotations of these nodes are fixed, except for the translation along the vertical axis at the top-end, for allowing the load application.

Two types of analyses are performed: linear eigenvalue analysis to calculate the buckling load, and non-linear analysis to determine the load-shortening curves, the post-buckling behavior and the influence of the initial geometric imperfections on the buckling load. It is important to highlight that the corrugated surface of the shells is not considered as initial geometric imperfections. The shape of the initial geometric imperfections of the non-linear analysis is taken equal to the first eigenmode of the linear eigenvalue analysis, and the amplitude is equal to 10% of the thickness.

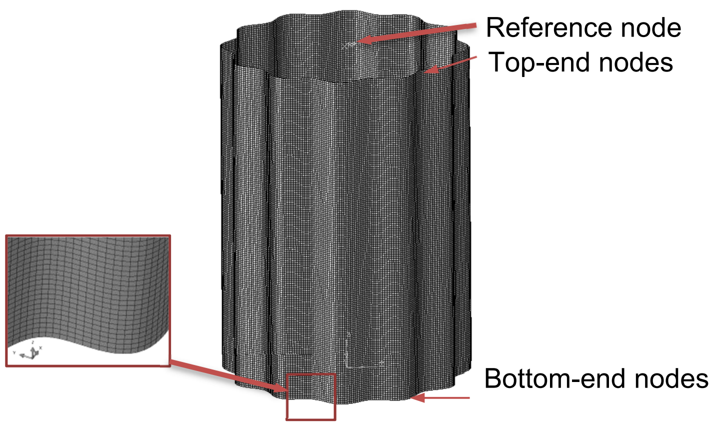

Figure 3 - Example of FE mesh of a corrugated shell.

3. Manufacturing and Testing of 3D-printed Shells

A few shells are manufactured using 3D-printing technology. In particular, the shells are fabricated using commercially available Creality Ender 3D-printer. A photo taken during manufacturing is shown in Figure 4. Three specimens of each shell type are fabricated.

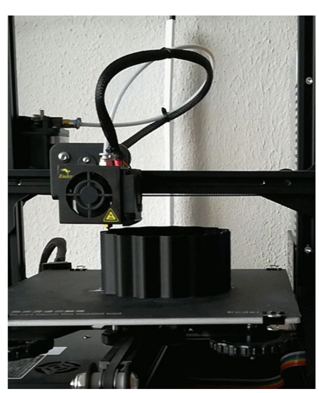

Figure 4 – 3D-printing of a corrugated shell.

The conventional cylindrical shells with circular section are taken as reference shell and serve to assess the performance of the corrugated shells. The 3D-printed shells manufactured in this phase have height of 170 mm, radius of 50 mm and wall thickness of 0.4 mm. The ratio between the radius and the thickness results equal to 125.

The shells with corrugated surface are manufactured considering 15 circumferential waves with a_n = 0.05. The two shell configurations have the same wall thickness, obtained by printing in spiralizer contour mode. Two 3D-printed shells, a reference shell and a corrugated shell, are shown in Figure 5.

All shells are then equipped with end reinforcement rings made of 6 mm Medium Density Fiberboard (MDF) milled by CNC machine. The reinforcement rings are bonded to the shell using polyvinyl acetate (PVA) adhesive.

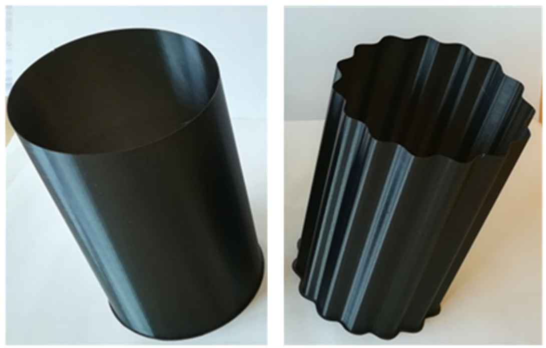

Figure 5 - Reference shell and corrugated shell.

The 3D-printed shells are tested in axial compression using a Zwick Z20 mechanical test machine with 20 kN load capacity. The test set-up is shown in Figure 6. The tests are performed placing the shells between two compression plates and operating in displacement control with loading rate of 0.5 mm/min. A Digital Image Correlation (DIC) system with two cameras is used to measure the axial displacement and the out-of-plane displacement of the shell, so to capture also the buckling mode. For being able to use the DIC system, the shells are painted white with contrasting black dotted pattern.

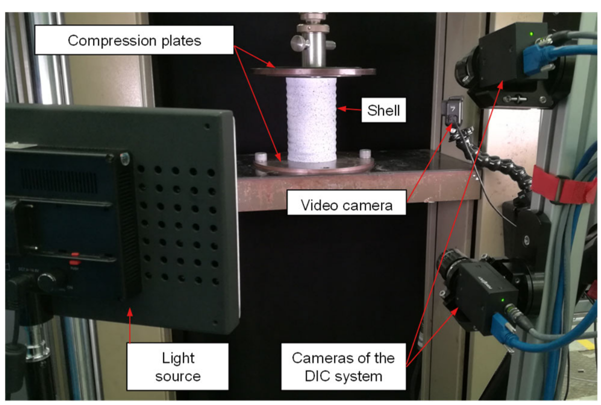

Figure 6 - Test set-up.

The load-shortening curves obtained during the tests of the three reference shells are reported in Figure 7. Good repeatability is measured for the stiffness of the shells. The average buckling load of the reference shells is 791 N with standard deviation of 36 N. The scatter in the measured buckling loads is due to the high sensitivity to the initial geometric imperfections and to the imperfections of the boundary conditions, as the reinforcement rings are bonded to the shells manually and the bond line might contain weaker spots or gaps invisible from outside. The reference shells lose load carrying capacity immediately after buckling. In the post-buckling field they present two rows of half-waves around the circumference.

The load-shortening curves obtained during the tests of the corrugated shells are reported in Figure 8. The average buckling load for these shells is 2143 N with standard deviation of 126 N. The buckling of the shell causes high strains in the axial direction because of the small radius of the corrugation wave which lead to local failure of the material. As this process does not happen simultaneously, the shells maintain some post-buckling load resistance.

Figures 7 and 8 present also the buckling load obtained by the linear eigenvalue analysis and the load-shortening curves obtained by the non-linear analysis. For both types of shells, the numerical load-shortening curves accurately predicts the stiffness and the buckling load of the shells. Also the post-buckling modes obtained by the FE analyses are very similar to those ones observed during the tests and measured using the DIC system.

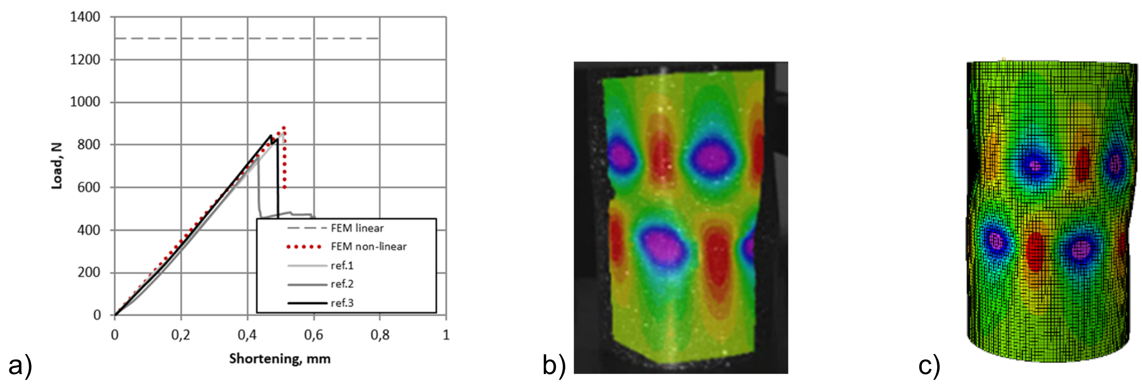

Figure 7 - Reference shell: a) Numerical-experimental comparison of load-shortening curves; b) Experimental post-buckling mode; c) Numerical post-buckling mode.

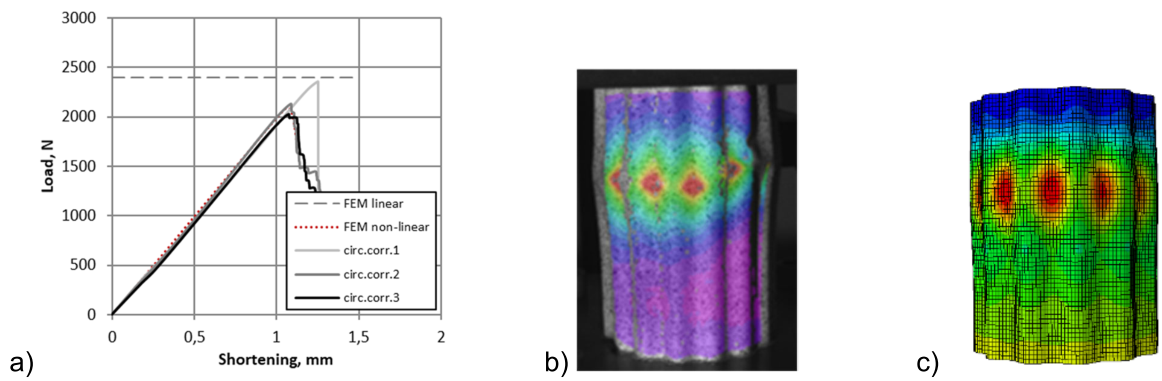

Figure 8 - Corrugated shell: a) Numerical-experimental comparison of load-shortening curves; b) Experimental post-buckling mode; c) Numerical post-buckling mode.

4. Optimization of Buckling Response

An optimization of the shells is performed employing a parametrical model generated by Python script and executed in Abaqus. The objective of the optimization is to maximize the buckling load P_{cr} maintaining the mass of the corrugated shells m_{corr} equal to the mass of the reference shell m_{ref}. Two parameters are selected for the optimization: the corrugation amplitude/radius ratio a_n and the number of the corrugation waves n.

For the optimization the radius of the shell is increased to 75 mm, maintaining the same height of 170 mm. In this way height/diameter aspect ratio is close to 1, and the larger radius allows more flexibility, because available printing nozzles have a thickness step of 0.1 mm. The wall thickness for the cylindrical shell with circular section taken as reference shell is set to 0.5 mm. Consequently, the corrugated shells present smaller thickness, to keep the mass of both shells the same.

In summary, the optimization formulation is defined maximizing the buckling load P_{cr} having $0.005 < a_n < 0.05$ and $5 < n < 25$, and maintaining $m_{corr} = m_{ref}$.

The simple optimization procedure is illustrated in Figure 9. The design of experiments (DoE) is generated using Latin Hypercube Sampling (LHS) with random design space filling criteria and 40 combinations. The FE models are generated in Python and the analysis are conducted in Abaqus as eigenvalue analyses. The responses provided by the FE analysis is approximated using locally weighted smoothing linear regression. The maximum value of the function is found using a solver from Matlab Optimization Toolbox.

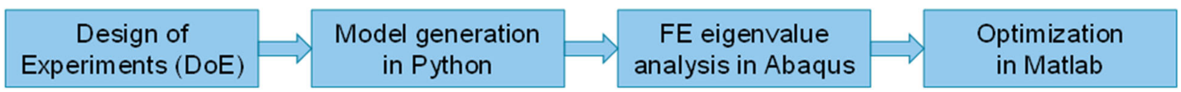

Figure 9 - Optimization procedure.

The approximation surface obtained for different number of the corrugation waves n and the amplitude/radius ratio a_n is shown in Figure 10. The highest linear buckling load of 3650 N is reached by the shell with 23 corrugation waves n and a_n value of 0.043. The wall thickness of the optimized shell is 0.41 mm, so that the mass is the same as the reference shell that presents wall thickness of 0.5 mm.

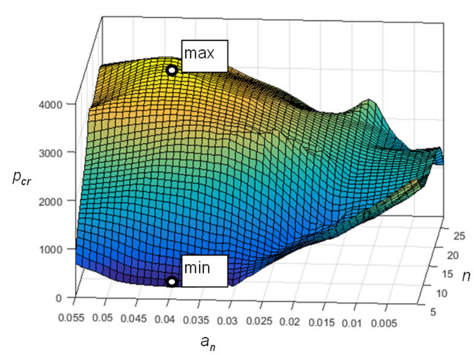

Figure 10 - Approximation surface of the optimization.

The optimized corrugated shell is then analyzed in more details performing a non-linear analysis, to determine also the influence of the geometrical imperfections. The shape of the initial geometric imperfections is taken equal to the first eigenmode of the linear buckling analysis, and three values of maximum imperfection amplitude are considered. The imperfection amplitude is related to the shell thickness t with ratios respect to the thickness equal to 0.1, 0.05 and 0.02.

The obtained load-shortening curves are presented in Figure 11. It is possible to see that both shells have the same stiffness due to equal cross section area, however the buckling load of the corrugated shell is significantly higher and less influenced by geometrical imperfection. The buckling load of the optimized corrugated shell is about 160% higher.

The evolution of the deformation of the optimized corrugated shell, as obtained from the FE nonlinear analysis, is reported in Figure 12.

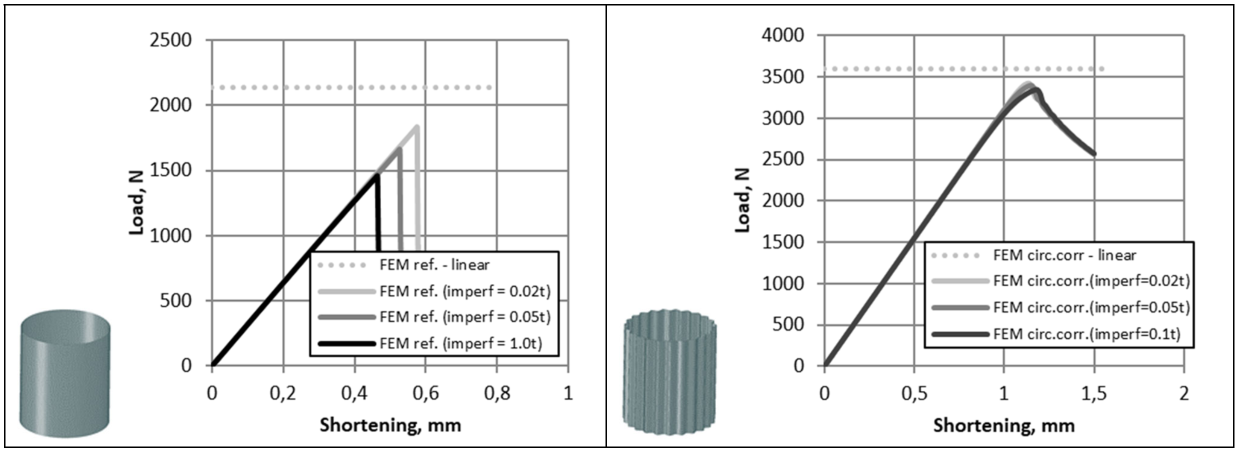

Figure 11 – Numerical load-shortening curves of the reference shell and of the optimized corrugated shell.

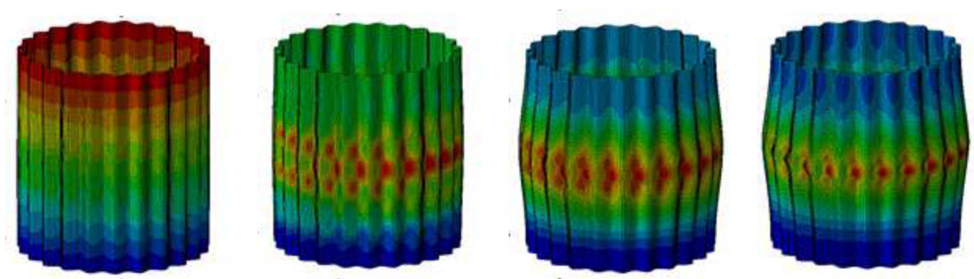

Figure 12 - Evolution from pre- to post-buckling of the optimized corrugated shell.

5. Concluding Remarks

The buckling response of corrugated cylindrical shells manufactured using 3D-printing technology has been investigated numerically and experimentally, to evaluate the influence of the corrugation parameters on the buckling load and the sensitivity towards initial geometric imperfections.

Initial 3D-printed shells were used to gain knowledge on the general behavior of 3D-printed shells and to validate the numerical models which were later used in the optimization. The numerical models well predicted the experimental behavior both for what concerns the load-shortening curves and the post-buckling modes.

A parametrical optimization of the corrugation parameters was then performed. The buckling load of the optimized corrugated shell results 160% higher compared to the reference cylindrical shell with circular section, maintaining the same mass. The corrugated shells resulted also less sensitivity to initial geometrical imperfections.

The knowledge acquired on the investigated small 3-D printed shells shows the potential 3D-printing technology as well as the possibility to optimize corrugated shells obtaining higher buckling load and less imperfection sensitivity, and can be useful for the design of new aerospace cylindrical shells.

6. Contact Author Email Address

Contact author: Prof. Chiara Bisagni, Delft University of Technology, Faculty of Aerospace Engineering, Delft, Netherlands

Mailto: c.bisagni@tudelft.nl

7. Copyright Statement

The authors confirm that they hold copyright on all of the original material included in this paper. The authors confirm that they give permission for the publication and distribution of this paper as part of the ICAS proceedings or as individual off-prints from the proceedings.

References

[1] Bisagni C and Cordisco P. An experimental investigation into the buckling and post-buckling of CFRP shells under combined axial and torsion loading. *Composite Structures*, Vol. 60, No. 4, pp. 391-402, 2003.

[2] Bisagni C. Composite cylindrical shells under static and dynamic axial loading: an experimental campaign. *Progress in Aerospace Sciences*, Vol. 78, pp. 107-115, 2015.

[3] Labans E, Bisagni C, Celebi M, Tatting B, Gürdal Z, Blom-Schieber A, Rassaian M and Wanthal S. Bending of composite cylindrical shells with circular cutouts: experimental validation. *Journal of Aircraft*, Vol. 56, No. 4, pp. 1534-1550, 2019.

[4] Uriol Balbin I, Bisagni C, Schultz MR and Hilburger MW, A scaling methodology applied to buckling of sandwich composite cylindrical shells. *AIAA Journal*, Vol. 58, No. 8, pp. 3680-3689, 2020.

[5] Ning X and Pellegrino S. Imperfection-insensitive axially loaded thin cylindrical shells. *International Journal of Solids and Structures*, Vol. 62, pp. 39-51, 2015.

[6] Ning X and Pellegrino S. Experiments on imperfection insensitive axially loaded cylindrical shells. *International Journal of Solids and Structures*, Vol. 115-116, pp. 73-86, 2017.

[7] Sowiński K. Buckling of shells with special shapes with corrugated middle surfaces – FEM study. *Engineering Structures*, Vol. 179, pp. 310-320, 2019.

[8] Wagner HNR, Petersen E, Khakimova R and Hühne C. Buckling analysis of an imperfection-insensitive hybrid composite cylinder under axial compression – numerical simulation, destructive and non-destructive experimental testing. *Composite Structures*, Vol. 225, p. 111152, 2019.

[9] White SC and Weaver PM. Towards imperfection insensitive buckling response of shell structures-shells with plate-like post-buckled responses. *The Aeronautical Journal*, Vol. 120, No. 1224, pp. 233–253, 2016.

[10] Labans E and Bisagni C. Buckling and free vibration study of variable and constant-stiffness cylindrical shells. *Composite Structures*, Vol. 210, pp. 446–457, 2019.

[11] Rashidi MRW, Frank GJ, Dohn T, Seifert R, Chapkin WA, Baur JW and Walgren PP. Biomimicry of the armadillo carapace for the design of bending cylinders for aerospace applications. *Proc AIAA SciTech Forum*, 10.2514/6.2019-1632, 2019.

[12] Liu Y, Zhang W, Zhang F, Lan X, Leng J, Liu S, Jia X, Cotton C, Sun B, Gu B and Chou TW. Shape memory behavior and recovery force of 4D printed laminated Miura-origami structures subjected to compressive loading. *Composites Part B: Engineering*, Vol. 153, No. 15, pp. 233-242, 2018.

[13] Gavioli M and Bisagni C. Teaching buckling of cylindrical shells through an effective laboratory demonstration. *Mechanics of Advanced Materials and Structures*, 2021.

[14] Labans E and Bisagni C. Buckling of 3D-printed cylindrical shells with corrugated surface. *Proc AIAA SciTech 2020 Forum*, 10.2514/6.2020-1925, Orlando, Florida, USA, 6-10 January 2020.

[15] Dessault Systems, Abaqus Analysis Guide, 2019.